Dalton Transactions

Accepted Manuscript

This article can be cited before page numbers have been issued, to do this please use: Q. wang, Z. zhou, C. C. Zhang and J. Gao, *Dalton Trans.*, 2016, DOI: 10.1039/C6DT00156D.

ROYAL SOCIETY OF CHEMISTRY

www.rsc.org/dalton

View Article Online
DOI: 10.1039/C6DT00156D

Molecular imaging of biothiols and in vitro diagnostics based on an organic chromophore bearing terbium hybrid probe

Zhan Zhou,[b] Qianming Wang,[a,b,c*], Cheng Cheng Zhang[d], Jinwei Gao[e]

a. Key Laboratory of Theoretical Chemistry of Environment, Ministry of Education, School of Chemistry & Environment, South China Normal University, Guangzhou 510006, China

b. School of Chemistry & Environment, South China Normal University, Guangzhou 510006, China

c. Guangzhou Key Laboratory of Materials for Energy Conversion and Storage Guangzhou 510006, P. R. China

d. Departments of Physiology and Developmental Biology, University of Texas, Southwestern Medical Center, Dallas, TX 75390-9133, USA

e. Institute for Advanced Materials, Academy of Advanced Optoelectronics, South China Normal University, Guangzhou 510006, P. R. China

* To whom the correspondence should be addressed. E-mail: qmwang@scnu.edu.cn
Tel: 86-20-39310258; Fax: 86-20-39310187

View Article Online
DOI: 10.1039/C6DT00156D

Abstract

For this research, A novel terbium-based luminescent hybrid inorganic/organic probe was designed and synthesized. Mesoporous silica nanospheres dispersed in water were used as the suitable host for the covalently linked lanthanide-containing organic structures. The lanthanide structure was linked to a sulfonate ester unit, which, in the presence of biothiols, was cleaved to result in terbium emission. The hybrid probe exhibited the capabilities of quantitative determination and detection limits for biothiols were presented (36.8 nM for Cys, 32.5 nM for GSH, and 34.7 nM for Hcy). Evaluation of luminescence changes in cell culture demonstrated that this smart probe is cell membrane permeable and selectively lights up in the presence of cysteine and glutathione in human embryonic kidney cells and human lung adenocarcinoma cells. This variation in the presence of biothiols can be controlled by the treatment with N-methylmaleimide. The narrow line-like bands and long-lived excited states of this terbium luminescent sensor permits discrimination from scattering signals and interfering fluorescence derived from biological tissues.

KEYWORDS: Terbium, Nanostructures, Probe, Bioimaging

View Article Online
DOI: 10.1039/C6DT00156D

INTRODUCTION

Rare earth elements have long been applied in the field of optical materials due to their narrow and characteristic emission signals derived from forbidden *f-f* electronic transitions. In order to achieve an efficient luminescent framework, the organic chromophore must absorb ultraviolet irradiation effectively and must efficiently transfer this energy to lanthanide centers. Therefore, numerous aromatic acids, β-diketones, and macrocylic ligands have been developed that form stable complexes with lanthanide ions and shield these cations from de-activation[1-4]. These light conversion molecular complexes have proven difficult to use in optical devices because of their poor thermal stabilities, photo-degradation, and low mechanical resistance. To avoid these issues, lanthanide organic/inorganic hybrid materials have been prepared [5-8].

Generally, direct doping with organometallic complexes results in problems such as clustering of emissive species and leaching of luminescent components due to weak interactions. Covalent anchoring of the organic functionalities to silica matrix enables preparation of high doping concentrations and homogenous dispersions [9-11]. These organically modified hybrid xerogels based on lanthanide emissions will be not only of fundamental interests, but also have superior applications in various fields like organic light emitting diodes, amplifiers or sensors [12,13]. As far as the inorganic hosts were concerned, hybrid networks composed of surfactant-templated porous organosilicas possess high surface area, large pore volume, and uniformly distributed pore size making them attractive matrices for the encapsulation of bulky organic moieties [14,15]. These embedded structures are readily constructed and have potential as luminescent probes [16-18].

View Article Online
DOI: 10.1039/C6DT00156D

In this work, a novel terbium-based luminescent hybrid inorganic/organic probe was designed and synthesized (Fig. 1). The achieved ligand **L** played dual roles. It can coordinate to lanthanide ions effectively and undergo sol-gel reactions based on polymerizable silylated groups (-Si(OEt)$_3$). In view of the molecular structure, it is accepted that two nitro- groups in DNBS have strong electron-withdrawing features and enormously disturb the electron distributions of pyridine derivative units in the fluorophore [19]. The photoinduced electron transfer affects the complexation with lanthanide ions and the hybrid nanosphere is weakly green fluorescent. But it has high affinity for thio-containing amino acids such as glutathione (GSH), cysteines (Cys) and Homocysteine (Hcy). The cleavage reaction of sulfonate ester by biothiols changes the electronic structure of the chromophore and in turn enhances the narrow green emissions. Although optical probes, including organic dyes, metal complexes, silver particles, and quantum dots, have been developed for the measurement of biothiols [20-25], the utilization of lanthanide luminescence as signaling moieties will gain advantages over the analogous sensing systems. The lanthanide line-like emission peaks (around 10 nm) could achieve desired signal to noise ratio compared to conventional fluorophores (emission bands covering more than 100 nm). Its long-lived excited states will avoid the side effects of auto-fluorescence and light scattering of biological tissues. Additionally, the metal emission might be highly sensitive to delicate changes in the coordination environments. More importantly, in this work, the selection of organoalkylsilanes as precursors to anchor the lanthanide organic complex inside the mesoporous framework will give rise to improved chemical or thermal stabilities. Here the first case of terbium-containing hybrid inorganic-organic thiols sensor has been described. The green luminescence of the probe

View Article Online
DOI: 10.1039/C6DT00156D

enables the quantitative assay of thiols in the nanomolar range with high selectivity. Validation of the probe in two live cell systems (HeLa and A549) demonstrates the potentialities of this sensor in medical diagnostics.

EXPERIMENTAL SECTION

Materials. Tb_4O_7 (99.9%) was purchased from Shanghai Yuelong. Terbium hydrochlorate was prepared by dissolving Tb_4O_7 in concentrated hydrochloric acid. Tetraethyl orthosilicate (TEOS, AR grade), cetyltrimethylammonium bromide (CTAB, AR grade), 3-(triethoxysilyl)propyl isocyanate (TEPIC, 96%), 4-hydroxypyridine-2,6-dicarboxylic acid (97%), tetramethylammonium hydroxide (TMAOH), tetramethylammonium chloride and N-Boc-ethylenediamine (98%) were purchased from J&K Scientific. N-methylmaleimide, glutathione (GSH), and amino acids, including cysteines (Cys), homocysteine (Hcy), alanine (Ala), arginine (Arg), aspartic acid (Asp), glutamic acid (Glu), glycine (Gly), histidine (His), leucine (Leu), lysine (Lys), methionine (Met), proline (Pro), serine (Ser), threonine (Thr), tryptophan (Trp), tyrosine (Tyr), and valine (Val), were purchased from Sigma-Aldrich. CellTiter 96® AQ_{ueous} One Solution Cell Proliferation Assay (MTS) was purchased from Promega. All the other reagents were purchased from Guangzhou Chemical Reagent Factory and used without further purification.

Synthesis of ligand (L). The synthesis of **L** is shown schematically in Figure S1, and the experimental details are as follows.

*Synthesis of compound **3***. Chelidamic acid hydrate (compound **1**) was reacted with methanol to form dimethyl 4-hydroxypyridine-2,6-dicarboxylate (compound **2**) based on

View Article Online
DOI: 10.1039/C6DT00156D

concentrated H_2SO_4. Compound **3** was obtained by the treatment of compound **2** with excess amounts of N-Boc-ethylenediamine. Compound **3** (yield: 72%) ^{1}H NMR (500 MHz, $CDCl_3$, ppm): 9.26 (s, 2H), 8.23 (s, 2H), 5.18 (s, 2H), 3.58 (m, 4H), 3.45 (m, 4H), 1.36 (s, 18H). MS (m/z): 468.6 [M + H].

*Synthesis of compound **4**.* Compound **3** (467 mg, 1.0 mmol) in dry CH_2Cl_2 (25 mL) and NEt_3 (300 μL) were mixed, and the solution was stirred in an ice-water bath for 15 min. 2,4-Dinitrobenzenesulfonyl chloride (532 mg, 2.0 mmol) was added, and the mixture was stirred for 3 h at room temperature. The solvent was evaporated, and the crude product was purified over a silica gel column (petroleum ether/ethyl acetate; 4:1, v/v) to obtain compound **4** as a yellow solid (yield: 52%). Compound **4** ^{1}H NMR (500 MHz, $CDCl_3$, ppm): 8.91 (s, 2H), 8.71 (d, J = 2.0 Hz, 1H), 8.58 (dd, J = 2.0 Hz, 2.5 Hz, 1H), 8.35 (d, J = 8.5 Hz, 1H), 8.15 (s, 2H), 5.25 (s, 2H), 3.62 (m, 4H), 3.46 (m, 4H), 1.38 (s, 18H). MS (m/z): 720.2 [M + Na].

*Synthesis of ligand (**L**).* Compound **4** was stirred with CH_2Cl_2/CF_3COOH (3:1, v/v) for 3 h at room temperature. The solvent was evaporated, yielding compound **5**. Compound **5** (385.5 mg, 0.75 mmol) was dissolved in 20 mL of anhydrous tetrahydrofuran under a steady flow of nitrogen, and TEPIC (592.8 mg, 2.4 mmol) was added with stirring. The mixture was refluxed under nitrogen for 6 h. The reaction was monitored by thin layer chromatography. Solvent was removed, and the product was purified on silica gel to give the ligand (**L,** yield: 57%). ^{1}H NMR (500 MHz, $CDCl_3$, ppm; Fig. S2): 8.93 (s, 2H), 8.71 (s, 1H), 8.62 (dd, J = 2.0 Hz, 2.5 Hz, 1H), 8.39 (d, J = 8.5 Hz, 1H), 8.18 (s, 2H), 5.78 (s, 2H), 5.36 (s, 2H), 3.82 (q, J = 8.5 Hz, 12H), 3.61 (m, 4H), 3.35 (m, 4H), 3.18 (t, J = 10.0 Hz, 4H), 1.62 (q, J = 8.5 Hz, 4H) 1.21 (t, J = 10.0 Hz, 18H), 0.65 (t, J = 10.0 Hz, 4H). MS (m/z): 992.5 [M + H]. Elemental

View Article Online
DOI: 10.1039/C6DT00156D

Analysis: Anal. Calcd for [$C_{37}H_{61}N_9O_{17}SSi_2$]: C, 44.79; H, 6.20; N, 12.71; S, 3.23. Found: C, 44.65; H, 6.13; N, 12.68; S, 3.30.

*Synthesis of the lanthanide complex (Tb**L**).* To prepare the terbium complex, **L** (198.4 mg, 0.2 mmol) was dissolved in 10 mL ethanol in a 25-mL round bottom flask, and 5 mL of a 0.04 M solution of $TbCl_3$ and ammonia (400 μL) were added with stirring. The mixture was refluxed for 3 h at 90 ^oC. The crude product was washed with ethanol and with water and then dried in vacuo overnight. The resulting precipitate was collected to give the desired terbium complex (yield: 82%). Elemental Analysis: Anal. Calcd for Tb**L**·$3H_2O$ [$C_{37}H_{61}N_9O_{17}SSi_2Tb·3H_2O$]: C, 36.88; H, 5.60; N, 10.46; S, 2.66. Found: C, 36.72; H, 5.72; N, 10.49; S, 2.58.

Synthesis of mesoporous silica nanoparticles (MSNs) and the hybrid material (H-MSN-Tb). Briefly, TEOS (0.1 ml) was mixed with 0.1 g CTAB, 0.6 g urea, and 30 ml water in an autoclave. The autoclave was sealed and hydrothermally heated to 180 ^oC. After 24 h, the autoclave was taken out of the oven and rapidly cooled under tap water. The precipitate was centrifuged and calcined at 550 ^oC for 5 h to remove the surfactant and yield the desired MSNs. To a suspension of MSNs (200 mg) in ethanol, 1 mL **L** in ethanol (0.5 M) and 500 μL of aqueous ammonia (30%) were added, and the suspension was stirred for 3 h. $TbCl_3$ solution (1 mL, 0.5 M) was added. After 12 h, the precipitate was centrifuged and redispersed in ethanol and water at least three times to remove unreacted **L** and lanthanide ions. The precipitate was dried in vacuo to give H-MSN-Tb.

Cell culture and MTS assay. HeLa cells (human embryonic kidney cells) were cultured in Dulbecco's modified medium (DMEM) supplemented with 10% fetal bovine serum (FBS)

View Article Online
DOI: 10.1039/C6DT00156D

and 1% penicillin. Cells were maintained at 37 °C in 5% CO_2. A549 cells (human lung adenocarcinoma cells) were cultured in Kaighn's Modification of Ham's F-12 supplemented with 10% FBS and 1% penicillin and maintained at 37 °C in 5% CO_2. To investigate cytotoxicity, cells were cultured in wells of 96-well plates for one day. Medium was then replaced with medium containing H-MSN-Tb (0, 5, 10, 20, 50, and 100 μg/mL), and cells were cultured for another 24 h. An aliquot of 20 μL MTT solution was added to each well. After incubated with 4 h, the absorbance at 490 nm was measured using a Polarstar microplate reader.

Cell imaging. For the experiments, cells were washed with medium, then incubated in medium containing H-MSN-Tb (100 μg/ml) for 2 hours. After washing twice with PBS, the cells were observed using a fluorescent microscope (Olympus BX50, Japan). For control experiments, cells were pretreated with N-methylmaleimide (100 μM) for 1 h and then incubated with H-MSN-Tb (50 μg/mL) for 2 h. When indicated, cells were incubated with 50 μM Cys or 50 μM GSH.

H-MSN-Tb characterization. ^{1}H-NMR spectra were recorded at 293 K using a Bruker Avance spectrometer (500 MHz) with TMS as an internal standard; all chemical shifts are reported in the standard notation of parts per million. Elemental analysis was carried out by a Vario EL cube machine (Elementar, Germany). Fluorescence emission and excitation spectra were measured using an Edinburgh FLS920 spectrometer. The absolute quantum yields were collected at room temperature through an integration sphere (Edinburgh FLS 920 spectrometer) method. FT-IR spectra were measured using a Shimadzu Prestige-21. LC-MS spectra were measured with a Thermo LC-MS equipment (LCQ- Advantage). Transmission

View Article Online
DOI: 10.1039/C6DT00156D

electron microscopy (TEM) was performed on a JEOL JEM-2100HR. Scanning electron microscopy (SEM) was measured on a Zeiss Ultra 55. The adsorption desorption isotherms of nitrogen were measured at 77 K using the ASAP2020M system. Thermogravimetric analyses (TGA) were carried out on a STA409PC system under air at a rate of 10 ^{o}C/min. HPLC analyses were performed on an Inertsil ODS-SP (5 μM, 4.6mm×250mm) column using a Shimadzu HPLC system that consists of two LC-20AT pumps and a SPD-20A UV-vis detector at 254 nm with acetonitrile/water (V/V = 4/1) containing 0.5 % trifluoroacetic acid as eluents at a flow rate of 0.8 mL/min. 10 μL was used for the injection volume.

RESULTS AND DISCUSSION

Synthesis of terbium inorganic/organic mesoporous hybrid nanosphere probe.

The terbium-based luminescent hybrid inorganic/organic probe is shown in Figure 1. Mesoporous silica nanospheres (MSN) dispersed in water were used as the host for the covalently linked lanthanide-containing organic structures. The MSN was derivatized with ligand (L), which chelates the lanthanide and contains a moiety reactive with thiols, and complexed with terbium to yield the hybrid probe H-MSN-Tb. The ligand was synthesized by conversion of chelidamic acid hydrate **1** to the ester **2** (Fig. S1). Compound **2** was reacted with N-Boc-ethylenediamine to produce amide **3**. An excellent electron acceptor, 2,4-dinitrobenzenesulfonyl (DNBS), was introduced into the organic framework to yield compound **4**. Following deprotection, 3-(triethoxysilyl)propyl isocyanate was grafted to the chromphore through amide linkages. This multifunctional precursor (**L**) was used to coordinate with terbium ions during a sol-gel process in order to prepare the mesoporous

View Article Online
DOI: 10.1039/C6DT00156D

hybrid material (Fig. 1).

Characterization of the probe.

The organic chromophore and the formation of the complex within the siloxane host were investigated by room-temperature infrared spectroscopy. The intense bands observed between 2800-3000 cm^{-1} were assigned to asymmetric and symmetric stretching vibrations of multiple CH_2 units in the ligand (Fig. 2a) and indicate that the 3-(triethoxysilyl)propyl isocyanate was successfully introduced into the organic framework. A broad signal detected at 1081 cm^{-1} was attributed to Si-O stretching vibration modes from the silica matrix (Fig. 2b). The successful grafting reaction was confirmed by two sharp peaks located at 1665 and 1554 cm^{-1} that correspond to C=O and N-H vibrations, respectively, due to urea units in the ligand. The C=O vibration mode was shifted to lower frequency ($\Delta\upsilon$ ca. 15 cm^{-1}) in the terbium complex than in the uncomplexed ligand, suggesting that all carbonyl moieties participate into the coordination with terbium ions.

Adsorption-desorption isotherms and pore size distribution curves of the uncomplexed and terbium containing hybrid material are shown in Fig. S3. Type IV isotherms were observed for both sample, indicating the existence of mesoporous ordered structures. The Brunauer-Emmett-Teller (BET) specific surface area and the pore volume measured for the terbium-containing material (529.6 $m^2\ g^{-1}$, 0.61 $cm^{-3}\ g^{-1}$, respectively) varied significantly from those of the uncomplexed sample (861.1 $m^2\ g^{-1}$, 0.95 $cm^{-3}\ g^{-1}$, respectively), suggesting that the terbium-containing organic structures were incorporated into the pores or the channels.

The thermogravimetric analysis (TGA) was carried out to determine thermal stabilities of

View Article Online
DOI: 10.1039/C6DT00156D

the organometallic complex and the mesoporous hybrid network (Fig. S4). At temperatures lower than 100 ^{o}C, weight loss was mainly due to desorption of water molecules. The second weight loss region between 200 and 500 ^{o}C is likely due to the decomposition of loaded organic structures. The pure metal complex was thermally unstable compared with that in the highly ordered mesostructured silica, indicating that the integration of the complex into the inorganic backbone improved durability. Above 500 ^{o}C, the weight loss is assumed to be due to decomposition of silica and the further condensation of silanols.

Representative SEM and TEM images of the probe are shown in Fig. 3. TEM micrograph displayed that the materials consist of well-preserved and uniform nanospheres. The narrow size distribution of the obtained granules was between 80 and 100 nm. Numerous well-ordered mesopores were found within the spherically shaped nanoparticles. Especially porous and hollow structures were identified in regular spheres.

Emission spectra in the presence of thiol and non-thiol biomolecules.

H-MSN-Tb exhibited a typical metal centered luminescence in HEPES buffer. Excitation of the organic chromophore at 284 nm (Fig. S5) resulted in a relatively weak green emission (Fig. S6). The narrow peaks were assigned to the electronic transitions from $^{5}D_{4}$ level to the $^{7}F_{J}$ levels (J = 6, 5, 4, and 3 at 490, 545, 583, and 621 nm, respectively). Upon addition of Cys, a dramatic emission intensity increase was observed depending on the time duration. The luminescence enhancement has reached a plateau within 15 min (Fig. S7). The relationship between pH value and the emission intensity of H-MSN-Tb with or without the biothiol treatment was shown in Fig. S8. When pH is above 5.0, the emission intensity of H-MSN-Tb was increased in the presence of Cys. In contrast, its fluorescence maintained relatively stable

View Article Online
DOI: 10.1039/C6DT00156D

in the absence of Cys at different pH environments. Therefore, H-MSN-Tb can be potentially used for the monitoring of thiols within physiological pH conditions.

The detection limit of H-MSN-Tb for thiols was investigated using fluorescence titration spectra. As shown in Fig. 4, the luminescence of H-MSN-Tb was dramatically enhanced with the addition of Cys. When the peak intensity at 545 nm was plotted against Cys concentration from 0 to 22 μM, the curve demonstrated an excellent linearity (correlation coefficient = 0.98). The plateau in the presence of Cys has been reached at the concentration of 22 μM. The detection of limit (36.8 nM) was calculated by the equation DL = 3×SD/S with a signal-to-noise ratio of 3 (DL means detection limit; S refers to the slope of the calibration curve; SD corresponds to standard deviation which was obtained by ten times parallel experiments of the blank sample). In addition, the quantum yields in the absence of Cys and in the presence of Cys were measured to be 0.35 % and 11.4 % respectively. Significant increase in luminescence intensity was also observed upon the addition of GSH to H-MSN-Tb (Fig. 5). A similar linear regression fitting equation has been generated with a 20-fold increase at the end of the titration (detection limit = 32.5 nM). Under the same conditions, the hybrid probe also demonstrated the analogous responses to Hcy, and the detection limit is 34.7 nM (Fig. S9). Therefore, the target probe can be used for quantitative determination of biothiols including GSH, Cys, and Hcy.

The selectivity was investigated by analysis of fluorescence responses in the presence of various amino acids. In the presence of up to 100 μM of other fifteen analytes (Ala, Arg, Asp, Glu, Gly, His, Len, Lys, Met, Pro, Ser, Thr, Trp, Tyr, and Val) there was little change in H-MSN-Tb emission (Fig. S10). Furthermore, common anions (F^-, Cl^-, Br^-, I^-, SO_4^{2-}, CO_3^{2-}, and

View Article Online
DOI: 10.1039/C6DT00156D

NO_3^-) or cations (K^+, Mg^{2+}, Ca^{2+}, Zn^{2+}, Al^{3+}, and Fe^{3+}) did not induce the emission intensity changes of the hybrid probe. However, when Cys was added into the above solution, it gave rise to a drastic enhancement effect which was similar to the addition of Cys alone (Fig. S11). Those results indicated that the hybrid probe can be used to selective detection of biothiols, and the recognize process was not influenced by the common competitive ions.

The above results suggest that lanthanide-based inorganic-organic mesoporous probe interacts specifically with biothiols, which induce cleavage of sulfonate ester. In the absence of the biothiol, the double nitro groups with potential electron-accepting features in ligand **L** pull electrons from pyridine ring to DNBS unit quenching its singlet emission and suppressing energy migration to terbium ions. In the presence of biothiols, the sulfonate ester bonds are cleaved and DNBS moiety is removed. The electronic structure of pyridine ring has been re-arranged and its emission is restored. So it could transfer ultra-violet energy to the central ions. Thus, only in the presence of biothiols was the terbium green emission at 545 nm detected. Although it was not convenient to apply routine molecular structure characterizations to study the hybrid inorganic-organic material (H-MSN-Tb) due to its solubility, we have found the useful information in the functional ligand **L** and its cleavage molecule **L'** (Fig. S12). Mass spectra results firmly supported the cleavage reaction. The mass signal assigned to the molecular weight of the cleaved compound (**L'**) was detected in the presence of Cys (Fig. S13). In addition, we also utilized HPLC to explore the reaction process of **L** with Cys. As shown in the following Fig. 6, ligand **L** gave a typical chromatographic band at 9.05 min. After the addition of Cys, this peak was reduced dramatically. A new peak at 6.92 min was observed and this product with the retention time of 6.92 min has been

View Article Online
DOI: 10.1039/C6DT00156D

confirmed to be ligand **L'** by mass result.

Use of H-MSN-Tb as a thiol sensor in cells.

Nanoscale hybrid sensors clearly have potential for use as diagnostic tools [26]. Thiol-containing amino acids like Cys and GSH play crucial roles in controlling regular cellular functions, and levels of these compounds are indicative of numerous diseases.[21] To determine whether our probe is useful in living cells, we performed experiment in two types of immortalized cells, HeLa and A549 cells. Probes used in vivo cannot be toxic to cells. Cytotoxicity of the H-MSN-Tb probe was determined using an MTS assay. Both HeLa and A549 cells were 95% viable at a concentration of 20 μg/mL H-MSN-Tb (Fig. 7). Under practical live cell imaging conditions of about 50 μg/mL probe, H-MNS-Tb also had very low cytotoxicity. These negligible toxicities suggest that these nanospheres are biocompatible and have potential for visualization of targets in cells.

Cell imaging under a fluorescence microscope revealed that both HeLa and A549 cells were stained intracellularly by H-MSN-Tb resulting in an intense green emission, indicating that the hybrid material penetrated cell membranes and was activated by thio-reactive components within cells (Figs. 8A and 9A). When cells were pretreated with the biothiol scavenger N-methylmaleimide prior to addition of H-MSN-Tb, the green luminescence was completely quenched (Figs. 8B and 9B). The significant fluorescence decrease was related to the removal of Cys and GSH by N-methylmaleimide. When GSH or Cys was added to cells pretreated with N-metylmaleimide, luminescence was observed again upon incubation with H-MSN-Tb (Figs. 8C, D and 9C, D). These results confirmed that the nanosphere-based lanthanide hybrid probe has potential as for use as a biosensor in living organisms.

View Article Online
DOI: 10.1039/C6DT00156D

CONCLUSIONS

A general strategy for the design and synthesis of novel lanthanide turn-on fluorescence probes has been described. The hybrid inorganic-organic network combines terbium coordinated pyridine derivative moieties as the fluorophore and 2,4-dinitrobenzenesulfonyl ester group as the recognition unit. The cleavage reaction releases the original terbium line-like green emissions and this sensor demonstrates rapid detection, excellent selectivity and high sensitivity for Cys and GSH in buffer solution. The low cytotoxicity displayed that the nano-sized luminescent probe has great potentials in visualizing biothiols efficiently in two live cell lines (including HeLa and A549). This switch-on type hybrid nano-sensor that enables clear observation of terbium emission changes will contribute to the new development of highly efficient smart probes in thiols sensing field.

ACKNOWLEDGMENTS

Q. M. appreciates National Natural Science Foundation of China (No. 21371063 and No.21328503), excellent university young scholar fund of Guangdong province (Yq2013053), Science and Technology Project in Guangzhou (2014J4100054), Natural Science Foundation of Guangdong (2015A030313378) and Guangdong Science and Technology plan (2013B010403025). J. W. thanks supports from National Natural Science Foundation of China (No.51571094) and Guangdong province fund (2014B09091505).

REFERENCES

View Article Online
DOI: 10.1039/C6DT00156D

(1) Parker, D.; Dickins, R. S.; Puschmann, H.; Crossland, C.; Howard, J. A. K. *Chem. Rev.* **2002**, *102*, 1977-2010.

(2) Bünzli J. C. G. *Chem. Rev.* **2010**, *110*, 2729-2755.

(3) Mahajan, R. K.; Kaur, I.; Kaur, R.; Uchida, S.; Onimaru, A.; Shinodab, S.; Tsukube, H. *Chem. Commun.* **2003**, *17*, 2238-2239.

(4) Almeida, P. F. A.; Klinowski, J.; Vilela, S. M. F.; Tomé, J. P. C.; Cavaleiro, J. A. S.; Rocha, J. *Chem. Soc. Rev.* **2012**, *41*, 1088-1110.

(5) Feng, J.; Zhang, H. J. *Chem. Soc. Rev.* **2013**, *42*, 387-410.

(6) Binnemans K. *Chem. Rev.* **2009**, *109*, 4283-4374.

(7) Nobre, S. S.; Cattoën, X.; Ferreira, R. A. S.; Carcel, C., Bermudez, V. D. Z.; Man, M. W. C.; Carlos, L. D. *Chem. Mater.* **2010**, *22*, 3599-3609.

(8) Li, H. R.; Lin, J.; Zhang, H. J., Fu, L. S.; Meng, Q. G.; Wang, S. B. *Chem. Mater.* **2002**, *14*, 3651-3655.

(9) Franville, A. C.; Zambon, D.; Mahiou, R. *Chem. Mater.* **2000**, *12*, 428-435.

(10) Wang, X. D.; Stolwijk, J. A.; Lang, T.; Sperber, M.; Meier, R. J.; Wegener, J.; Wolfbeis, O. S. *J. Am. Chem. Soc.* **2012**, *134*, 17011-17014.

(11) Duarte, A. P.; Gressier, M.; Menu, M. J.; Dexpert-Ghys, J.; Caiut, J. M. A.; Ribeiro, S. J. L. *J. Phys. Chem. C* **2012**, *116*, 505-515.

(12) Armelao, L.; Quici, S.; Barigelletti, F.; Accorsi, G.; Bottaro, G.; Cavazzini, M.; Tondello, E. *Coord. Chem. Rev.* **2010**, *254*, 487-505.

(13) Ai, K. L.; Zhang, B. H.; Lu, L. H. *Angew. Chem. Int. Ed.* **2009**, *48*, 304-308.

(14) Yu, Q. Y.; Hui, J. F.; Wang, P. P.; Xu, B.; Zhuang, J.; Wang, X. *Nanoscale* **2012**, *4*,

View Article Online
DOI: 10.1039/C6DT00156D

7114-7120.

(15) Zhang, K.; Xu, L. L.; Jiang, J. G.; Calin, N.; Lam, K. F.; Zhang, S. J.; Wu, H. H.; Wu, G. D.; Albela, B.; Bonneviot, L.; Wu, P. *J. Am. Chem. Soc.* **2013**, *135*, 2427-2430.

(16) Balaji, T.; Sasidharan, M.; Matsunaga, H. *Analyst* **2005**, *130*, 1162-1167.

(17) Zhou, Z.; Zheng, Y. H.; Wang, Q. M. *Inorg. Chem.* **2014**, *53*, 1530-1536.

(18) Dufaud, V.; Beauchesne, F.; Bonneviot, L. *Angew. Chem. Int. Ed.* **2005**, *44*, 3475-3477.

(19) Yu, C. M.; Zeng, F.; Luo, M.; Wu, S. Z. *Nanotechnology* **2012**, *23*, 305503.

(20) Tanaka, F.; Mase, N.; Barbas, C. F. *Chem. Commun.* **2004**, *15*, 1762-1763.

(21) Jung, H. S.; Chen, X. Q.; Kim, J. S.; Yoon, J. *Chem. Soc. Rev.* **2013**, *42*, 6019-6031.

(22) Zhang, N.; Qu, F.; Luo, H. Q.; Li, N. B. *Biosens. Bioelectron.* **2013**, *42*, 214-218.

(23) Zhang, W. Z.; Zhang, R.; Zhang, J. M.; Ye, Z. Q.; Jin, D. Y.; Yuan, J. L. *Anal. Chim. Acta* **2012**, *740*, 80-87.

(24) Zhang, J.; Shibata, A.; Ito, M.; Shuto, S.; Ito, Y.; Mannervik, B.; Abe, H.; Morgenstern, R. *J. Am. Chem. Soc.* **2011**, *133*, 14109-14119.

(25) Sun, W.; Li, W. H.; Li, J.; Zhang, J.; Du, L. P.; Li, M. Y. *Tetrahedron* **2012**, *68*, 5363-5367.

(26) Quang, D. T.; Kim, J. S. *Chem. Rev.* **2010**, *110*, 6280-6301.

View Article Online
DOI: 10.1039/C6DT00156D

Figure captions

Figure 1. Schematic illustration of responsive MSN-based sensor H-MSN-Tb.

Figure 2. IR spectra of ligand **L** (solid line) and H-MSN-Tb (dotted line).

Figure 3. TEM (top) and SEM (bottom) images of H-MSN-Tb.

Figure 4. Emission spectra of H-MSN-Tb (50 μg/mL) upon addition of Cys (from 0 to 22 μM) in 30 mM HEPES buffer, pH 7.0 (λ_{ex}= 284 nm). Inset: Relative intensity of H-MSN-Tb at 545 nm as a function of Cys concentration from 2 to 22 μM. Detection limit: 36.8 nM.

Figure 5. Emission spectra of H-MSN-Tb (50 μg/mL) upon addition of GSH (from 0 to 20 μM) in 30 mM HEPES buffer, pH 7.0 (λ_{ex}= 284 nm). Inset: Relative intensity of H-MSN-Tb at 545 nm as a function of GSH concentration from 2 to 20 μM. Detection limit: 32.5 nM.

Figure 6. Typical HPLC of chromatogram of ligand **L** (20 μM, a) and ligand **L** (20 μM) incubated with Cys (40 μM) for 30 min (b). Peaks in the chromatograms were detected by monitoring the absorption at 254 nm. The mobile phase was 4/1 acetonitrile/water containing 0.5 % trifluoroacetic acid at a flow rate of 0.8 mL/min.

Figure 7. Viability of HeLa cells (red bar) and A549 cells (black bar) after 24 h in the presence of indicated concentrations of H-MSN-Tb.

Figure 8. (A) Fluorescence image of HeLa cells incubated with 50 μg/mL H-MSN-Tb for 2 h. (B) Fluorescence image of HeLa cells pretreated with 100 μM N-methylmaleimide for 1 h, then incubated with 50 μg/mL H-MSN-Tb for 2 h. (C) Fluorescence image of HeLa cells pretreated with 100 μM N-methylmaleimide for 1 h, then incubated with 50 μM Cys and 50 μg/mL H-MSN-Tb for 2 h. (D) Fluorescence image of HeLa cells pretreated with 100 μM N-methylmaleimide for 1 h, then incubated with 50 μM GSH and 50 μg/mL H-MSN-Tb for 2

View Article Online
DOI: 10.1039/C6DT00156D

h.

Figure 9. (A) Fluorescence microscope images of A549 cells incubated with 50 μg/mL H-MSN-Tb for 2 h. (B) Fluorescence images of A549 cells pretreated with 100 μM N-methylmaleimide for 1h, then incubated with 50 μg/mL H-MSN-Tb for 2h. (C) Fluorescence microscope images of A549 cells pretreated with 100 μM N-methylmaleimide for 1 h, and then incubated with 50 μM Cys and 50 μg/mL H-MSN-Tb for 2 h. (D) Fluorescence microscope images of A549 cells pretreated with 100 μM N-methylmaleimide for 1 h, and then incubated with 50 μM GSH and 50 μg/mL H-MSN-Tb for 2 h.

View Article Online
DOI: 10.1039/C6DT00156D

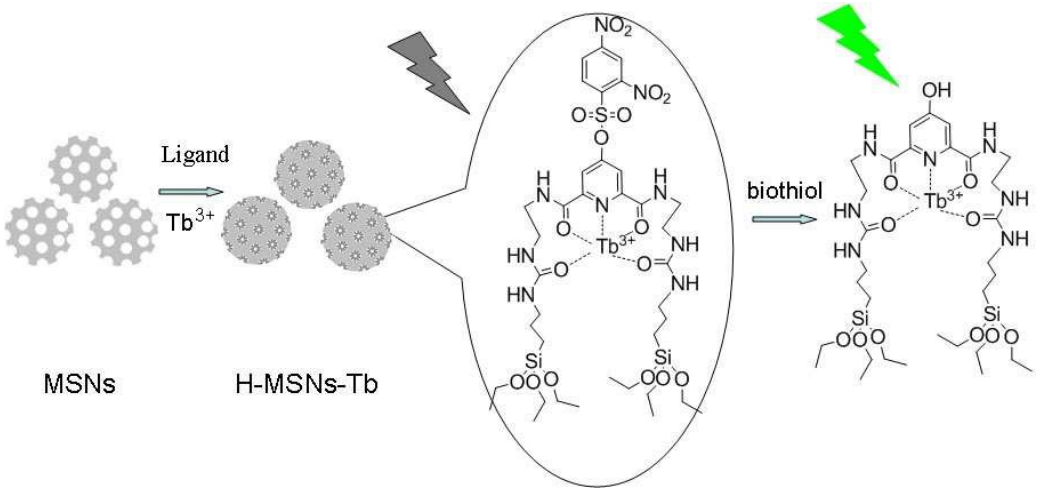

1

2 Fig. 1

3

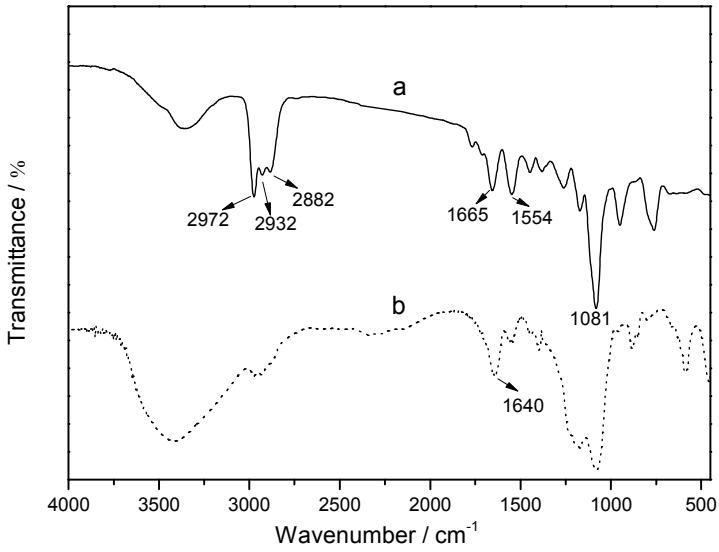

4

5 Fig. 2

6

View Article Online
DOI: 10.1039/C6DT00156D

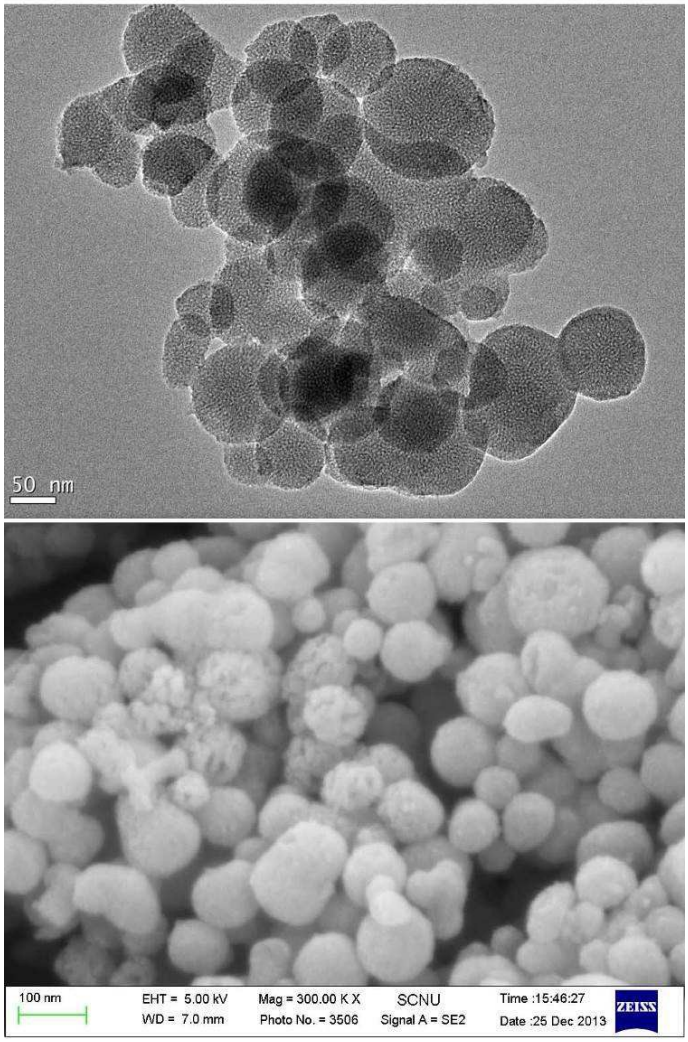

Fig. 3

View Article Online
DOI: 10.1039/C6DT00156D

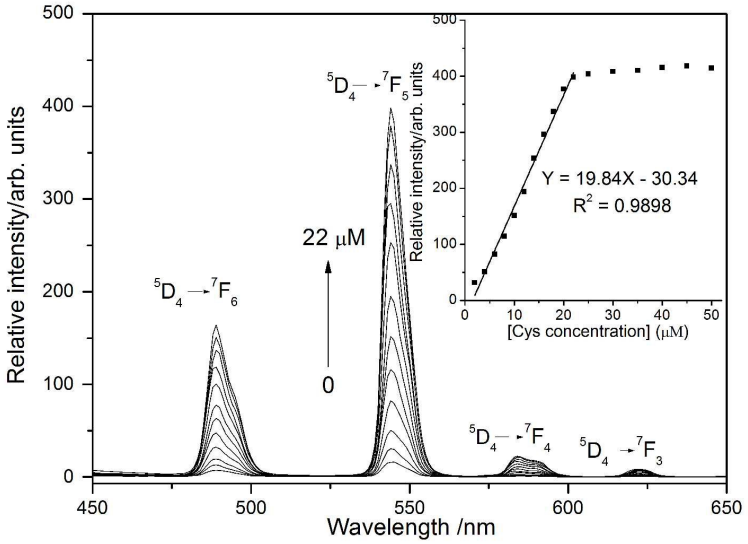

Fig. 4

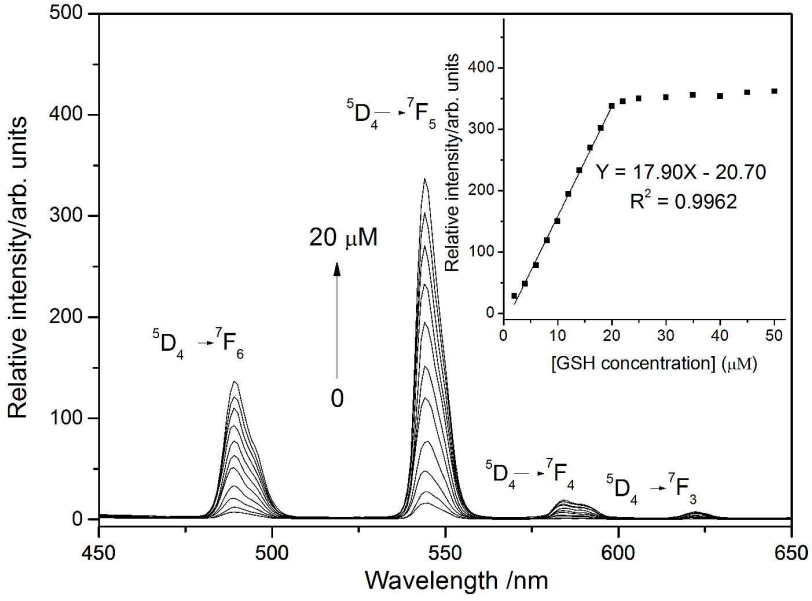

Fig. 5

View Article Online
DOI: 10.1039/C6DT00156D

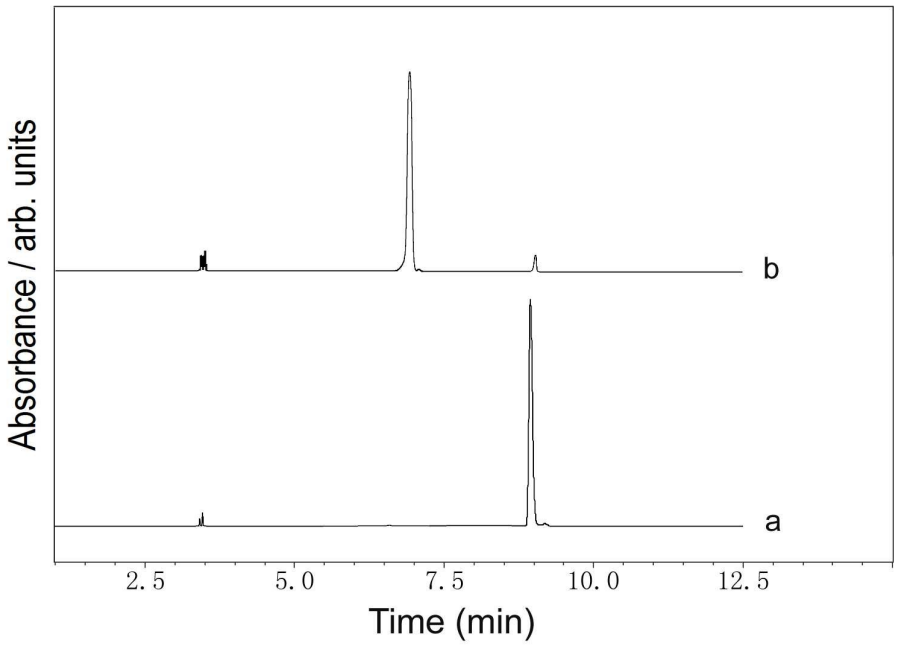

Fig. 6

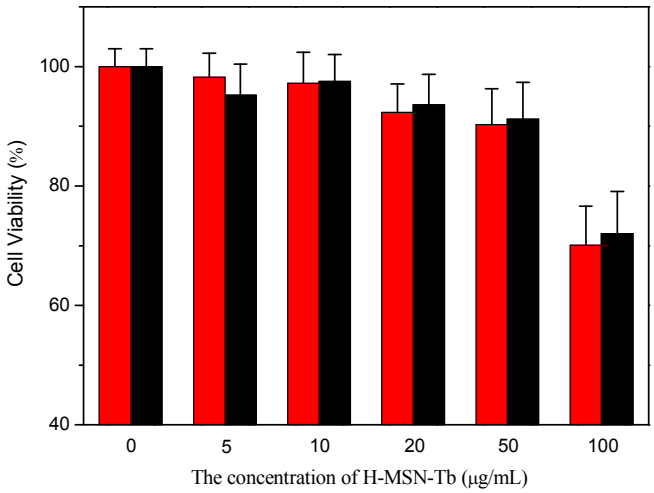

Fig. 7

View Article Online
DOI: 10.1039/C6DT00156D

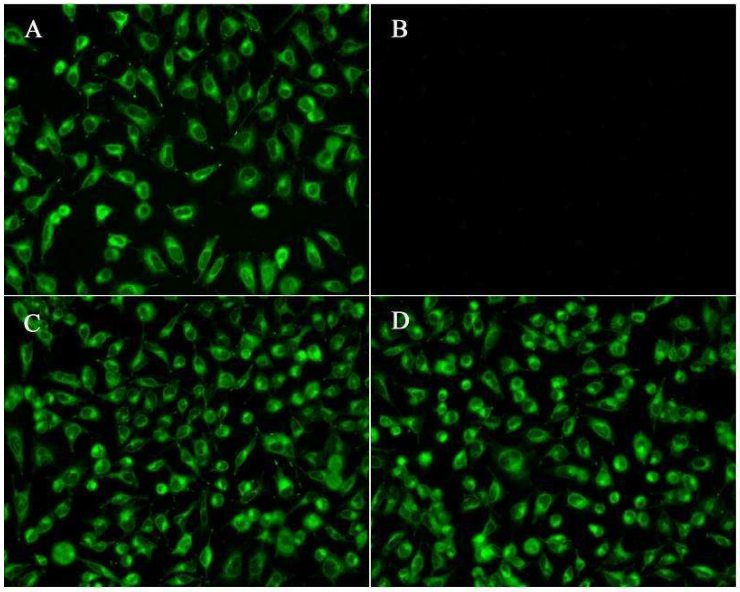

Fig. 8

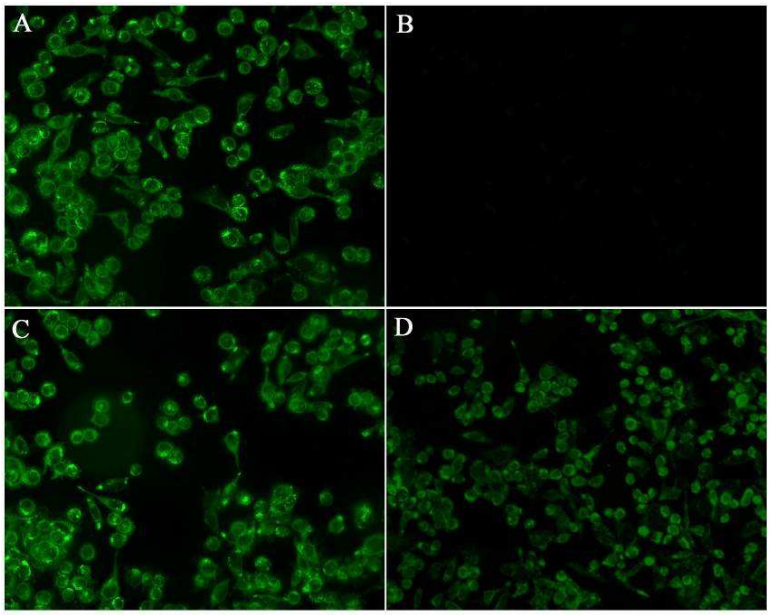

Fig. 9